Proton Pumping Mechanism in Cytochrome c Oxidase†

Per E. M. Siegbahn and Margareta R. A. Blomberg*

Department of Physics, Albanova, and Department of Biochemistry and Biophysics, Arrhenius Laboratory, Stockholm University, SE-106 91, Stockholm, Sweden

Received: February 25, 2008; Revised Manuscript Received: June 2, 2008

Two different issues, important for the pumping mechanism of cyctochrome c oxidase, have been addressed in the present study. One of them concerns the nature of two key proton transfer transition states. A simple electrostatic model is used to suggest that the transition state (TS) for transfer to the pump-site should be positively charged, while the one for transfer to the binuclear center should be charge-neutral. The character of the former TS will guarantee that the protons will be pumped to the outside and not return to the inside, while the neutral character of the latter one will allow transfer with a sufficiently low barrier. In the simple electrostatic analysis, leading to this qualitative picture of the pumping process, the results from the kinetic experiments are strictly followed, but it is at least as important to follow the fundamental requirements for pumping. In this perspective, the uncertainties in the quantitative analysis should be rather unimportant for the emerging qualitative picture of the pumping mechanism. The second problem addressed concerns the purpose of the K-channel. It is argued that the reason for the presence of the K-channel could be that protons cannot pass through the binuclear center at some stage of pumping. Barriers and water binding energies were computed using hybrid density functional theory (DFT) to investigate this question.

I. Introduction

Eukaryotic cytochrome c oxidase is situated at the end of the respiratory chain in the mitochondrial membrane. It converts the energy released when dioxygen is reduced to water into a electrochemical gradient across the membrane.[1] The general present view is that for each electron transferred to the enzyme from cytochrome c on the P-side (positive side of the membrane), one proton is taken up from the N-side (negative side) for the reduction chemistry and one proton is translocated from the N-side to the P-side. Understanding how the enzyme is able to use the chemical energy to move protons against the gradient, while at the same time preventing protons from going with the gradient the opposite way, has proved extremely difficult and remains one of the major unsolved problems in biochemistry. All indications are that the gating mechanism used is unique for this enzyme.

The X-ray structures of both the mammalian and the bacterial enzyme have been known at reasonably high resolution for about ten years.[2,3] The most essential structural elements are shown in Figure 1. The electron sent from cytochrome c is first accepted by Cu_A, a binuclear copper center close to the P-side of the membrane. The electron is then transferred to heme a and then further to the binuclear center (BNC) where dioxygen binds. BNC is formed by another heme group, heme a_3, and a mononuclear copper complex, Cu_B, with three histidine ligands. Dioxygen binds between iron and copper. Most of the protons taken up from the N-side, both for the dioxygen reduction chemistry and for pumping, are transferred in the D-channel ending at a critical glutamic acid, Glu278. At this residue, the protons can take two directions, toward the BNC or toward the P-side for pumping. It is generally assumed that the latter protons stay at a pump-site before being pumped to the P-side. A commonly suggested pump-site is propionate A (Prop-A) of heme a_3, shown in the figure. A schematic picture of electron and proton flow is shown in Figure 2. The positions of two important transition states, to be discussed below, are also indicated in the figure: one close to Glu278 and one close to the P-side.

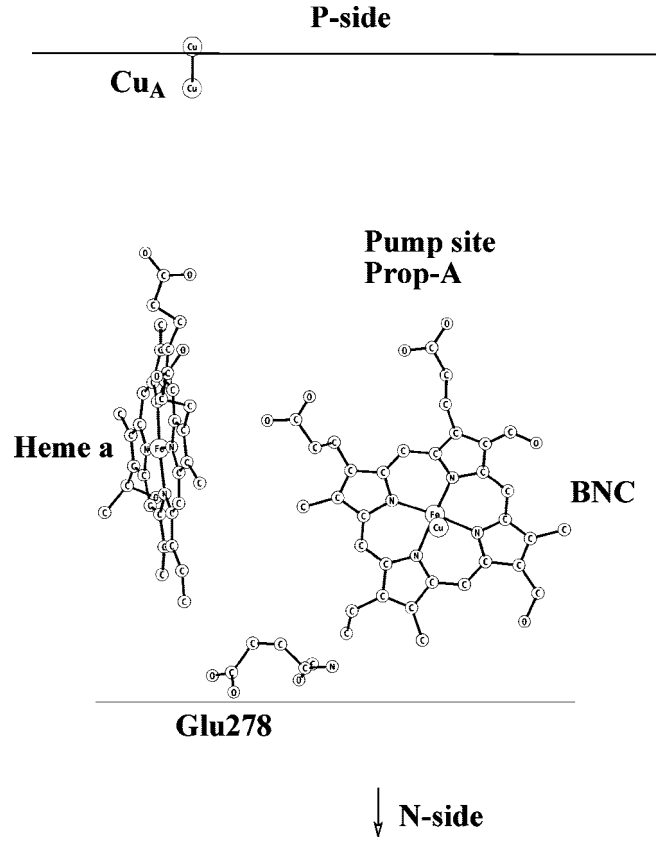

Figure 1. X-ray structure of cytochrome c oxidase showing the most important cofactors.

* Corresponding author. Email: mb@physto.se.

† Part of the "Sason S. Shaik Festschrift".

10.1021/jp801635c CCC: $40.75
Published on Web 09/06/2008

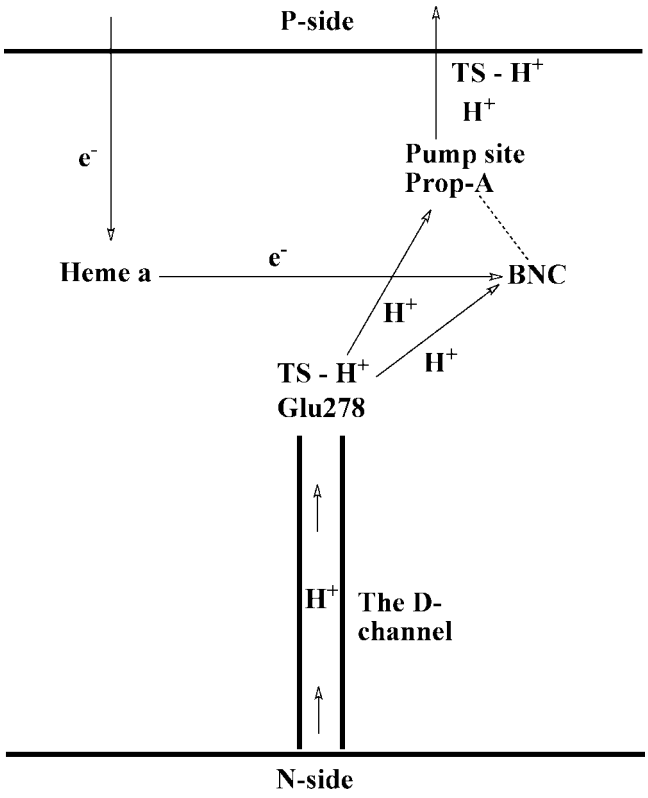

Figure 2. Schematic picture of electron and proton flow in cytochrome c oxidase.

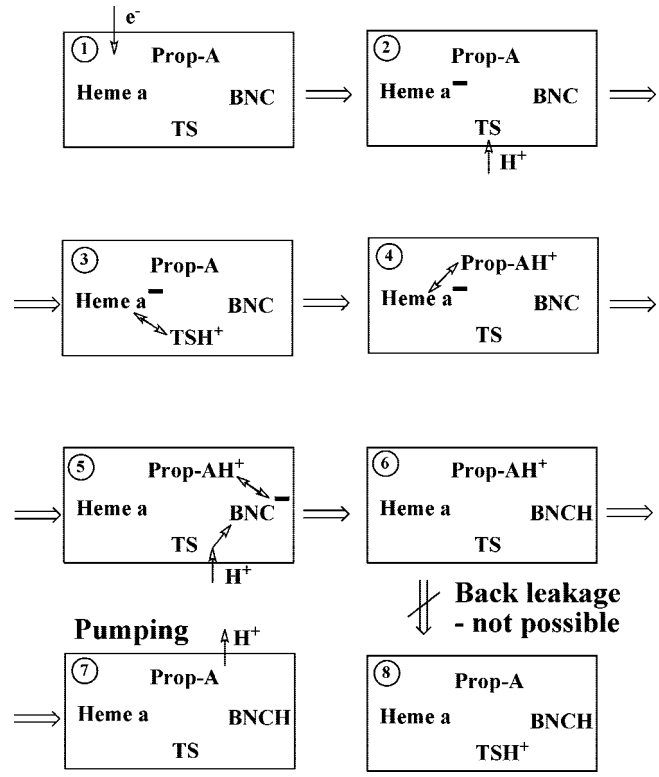

Figure 3. Model for pumping discussed in the previous study, highlighting the electrostatic mechanism for gating the protons toward the P-side of the membrane. The doublesided arrows indicate a mutual electrostatic stabilization.

A major step toward a better understanding of the pumping mechanism was taken recently, both experimentally and theoretically. Experimentally, a kinetic study of one of the four cycles of dioxygen reduction, the so-called **O** to **E** transition, was performed in which each intermediate appearing from electron and proton transfer in the enzyme was time-resolved and analyzed.[4] Two different diagrammatic analysis shed further light on the pumping process.[5,6] The general picture obtained in these two latter studies was similar but different on essential points. The different steps, as described in one of the papers,[5] is shown in Figure 3. In this mechanism, derived from the kinetic experiments, a positively charged transition state near Glu278 plays a fundamental role. In **1** to **2**, an electron is transferred to heme a, coupled with a proton uptake from the N-side to the Glu278 transition state. The positively charged TS is thus stabilized by the negative charge on heme a, indicated by a doublesided arrow in **3**. In **4**, the proton has continued to the pump-site, concluded to be Prop-A, where the proton is again stabilized by the electron on heme a. The next step is an electron transfer from heme a to the BNC in **4** to **5**. The proton on the pump-site is still stabilized by the electron. In **5** to **6**, the negative charge on the BNC triggers another proton uptake from the N-side. A TS is passed before the proton reaches the BNC. At **6**, one of the most critical stages of the pumping process is reached, since there is no longer any electrostatic stabilization of the proton at the pump-site. The energy is unstable and the proton has two choices. Thermodynamically, the proton would prefer to go to the N-side but is forced to the P-side. The reason for this is that the TS, which the proton has to pass in order to reach the N-side, is no longer electrostatically stabilized by any negative charge, and is therefore too high. The reaction path from **6** to **8** is thus no longer allowed (it is too slow on the timescale of the pumping process), and the proton instead has to follow the path from **6** to **7** after which the pumping is completed. The positive character of the TS for proton transfer from the N-side to the pump-site is therefore the most important finding in that analysis. The other study analyzing the kinetic experiments did not reach the same conclusion, but a neutral TS was suggested, in which a charge separation of Glu278 occurs forming $GluO^- \cdots H_3O^+$.[6] The advantage with the latter analysis is that a clear role is given for Glu278, missing in the analysis in Figure 3. The drawback is that the gating of the protons toward the P-side can not be as easily explained.

In the study described by the scheme in Figure 3, one of the main problems of describing a working pumping process was solved by introducing a positively charged TS close to Glu278. As already indicated in that study, a few important problems still have to be removed before a fully satisfactory scheme is found. One of them is a definite role of Glu278. Even though the suggested TS should be close to Glu278, it is not clear that a glutamic acid is needed to form such a TS. A good explanation for the unusually high pK_a of this residue is also missing. Furthermore, in the quantitative analysis of the kinetic experiments, an explanation has to be provided for the relatively low barrier found experimentally for the second proton, the one going to the BNC. Experimentally, the first proton, the one going to the pump-site in **3**, experiences a barrier of 12.2 kcal/mol (from transition state theory).[4] The one going to the BNC in **5** has a barrier of 13.2 kcal/mol. It should be noted that in the analysis performed here using transition state theory, it is only the exponential dependence of the barrier heights that matters. An uncertainty in the pre-exponential factor would cancel in all comparisons. An important difference between **3** and **5** is that in **5** there is a proton on the pump-site. The estimated repulsive effect on the barrier from this proton should be about 5 kcal/mol, not only 1 kcal/mol (13.2−12.2 kcal/mol), if a positively charged TS is assumed. In the present paper these problems are addressed and a solution is suggested. It should

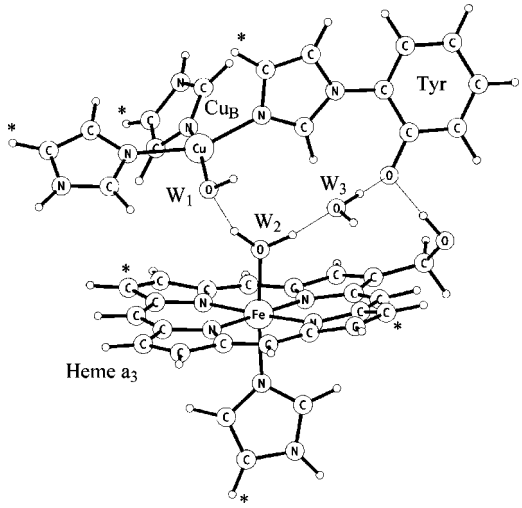

Figure 4. Model used in the calculations on the binuclear center, BNC. The atoms marked with an asterisk are frozen in the geometry optimizations.

here be noted that with the type of positive transition state suggested here for the proton transfer to the pump-site, the fact that the experiments were performed at pH = 8 has to be taken into account, which was disregarded in the previous study. This means that for the proton transfer to the pump-site, the barrier at pH = 7 should be 10.8 kcal/mol, a value that is used in the present study. As will be seen below, for the proton transfer to the BNC, another type of transition state will be suggested, which is not affected by the pH. The results in the present study are mainly based on experimental measurements and simple electrostatic evaluations. The quantitative values for the electrostatic interactions will clearly have uncertainties. However, the important point is that this analysis gives a qualitative picture of proton pumping, which should be rather independent of these uncertainties. In section IV, some details of the proton motion are also investigated using quantum chemical model calculations.

Since the proton pumping in cytochrome c oxidase is one of the most important issues in bioenergetics, much efforts have been put into the elucidation of the mechanism. Many suggestions based on different types of experimental information have been made.[7−16] Several theoretical investigations have also been performed using different techniques, ranging from Monte Carlo simulations to quantum mechanical calculations.[17−26]

II. Model Calculations

Hybrid density functional theory calculations have been performed on models of the binuclear center, BNC, to investigate some aspects of the proton transfer processes occurring within the binuclear center; see section IV below. The model used in the present study, shown in Figure 4, is based on one of the available X-ray structures.[2] Heme a_3 is modeled as an essentially unsubstituted porphyrin, only the farnesyl hydroxyl group is kept, since it forms a hydrogen bond to a tyrosine which is included in the model. The three histidine ligands of Cu_B and the axial ligand of heme a_3 are modeled as imidazoles. The tyrosine residue cross-linked to one of the copper−histidine ligands is proposed to be involved in the chemistry, and it is therefore also included in the model, as a phenol group. To mimic the constraints exerted by the surrounding protein, certain atoms in the model are frozen from the X-ray structure. The hydrogen atom on each imidazole, representing the connection to the backbone, and two carbon atoms on the porphyrin are frozen; see Figure 4. No atom on the tyrosine is frozen, but its motion is restricted by the cross-link to the histidine. The same model has been used in a previous study,[27] while similar but larger models of different sizes have been used in several previous studies.[17−19,28]

The B3LYP hybrid functional is used in the calculations. The geometries are optimized using the lacvp basis,[29] which is of double-ζ quality, and the final energies are evaluated using the lacv3p* basis,[29] which is of triple-ζ quality with polarization functions on all heavy atoms. The self-consistent reaction field (SCRF) method implemented in Jaguar was used to evaluate electrostatic effects from the surrounding protein,[30,31] using an effective dielectric constant $\epsilon = 4$ and a probe radius = 2.5 Å.

Several benchmark tests on the accuracy of the B3LYP functional have been performed.[32] On the basis of those results, an average error of 3−5 kcal/mol is expected for the computed relative energies for transition metal containing systems.[33] There are indications that the reparameterized B3LYP* functional, which uses 15% Hartree−Fock exchange as compared to the 20% used in the original functional, gives a better description of relative energies in transition metal containing systems.[34,35] Therefore relative energies have also been evaluated using the B3LYP* functional.

An important issue in the present study is the binding energy of water molecules to the binuclear center, and the relevant value is the binding energy relative to bulk water. The value for the binding energy of one water molecule in bulk water is taken to be 14 kcal/mol, which thus has to be subtracted from the water binding energy directly computed. In this context, the computed water binding energy is obtained by including dielectric effects for the model complex (with and without the water molecule) but not for the free water molecule.

III. Mechanism for Proton Pumping

In order to proceed from the previous study on proton pumping,[5] the different interaction energies measured and assumed have to be clarified. Experimentally,[4] a proton moves from the N-side to the pump-site when an electron reaches heme a from the Cu_A. Since the electron on Cu_A disappears, this reaction step has to be exergonic by at least 3 kcal/mol. Other experimental observations combined with the experimental driving force require that the exergonicity is not greater than 5 kcal/mol. In the previous paper, it was assumed to be 5.0 kcal/mol to match other requirements for the pumping process. Assuming a point charge representation of both the heme (iron) and the pump-site (an oxygen of Prop-A) leads to a dielectric constant of 3.3. This is by normal standards an unusually low dielectric constant. Still, in the present paper, this value has been used for all interactions. A possible alternative, not explored here, is to use the experimentally derived interaction energies (without any use of dielectric constant) for the interactions where the electrons on the metal centers are discussed, but to use a much higher dielectric constant for the other interactions involved. That procedure would only modify one of the interaction energies, the one between Glu278 and Prop-A, and would in fact make the previous pumping mechanism fully workable without further change, something which will be discussed in a future paper.

The main results of the previous study on the proton pumping mechanism[5] was given in the Introduction. In short, the analysis led to a solution of the gating problem, which forces the proton to go to the P-side rather than back to the N-side at a critical stage; see Figure 3. This was achieved by making the transition state positively charged. However, if a similar type of transition state is assumed for the proton going to the BNC (using ϵ =

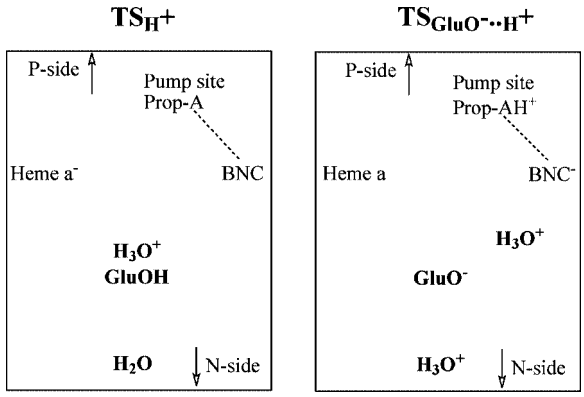

Figure 5. Two extreme types of proton transfer transition states.

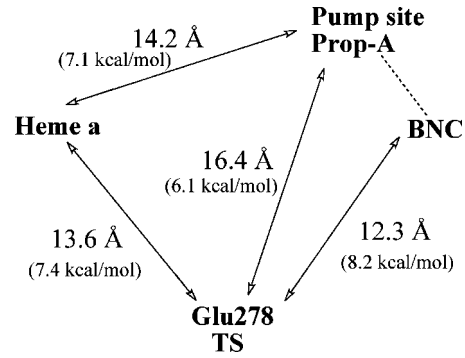

Figure 6. Relevant distances for the discussion of pumping. Corresponding interaction energies, computed with $\epsilon = 3.3$, are given in parenthesis.

3.3; see above), the barrier becomes too high for matching the experimental rate. Also, the type of charged transition state suggested does not give a clear role for Glu278, which is experimentally known to be extremely important for the pumping process.

In order to approach a unified solution to the pumping mechanism, the transition states for proton motion from the N-side toward the pump-site, and to the BNC, are considered more in detail. The positively charged TS discussed previously can then be described as in Figure 5 left, representative of proton motion to the pump-site. A proton has moved from the N-side and the TS can be regarded as the point where the proton passes Glu278. A slightly different description of the same process is to say that it starts by a very short charge separation between the proton and Glu278 to $GluO^-\cdots H_3O^+$, with an immediate reprotonation of the glutamate from the N-side. Another extreme of a similar type of TS is shown on the right in the figure and is representative for proton motion to the BNC. In this case, there is no immediate reprotonation but the proton coming from the N-side is still far away from Glu278 at the point where the TS is reached. The most important difference between the left and right portions of the figure is that the electron has moved from heme a to the BNC. In the case on the right, the electron gives a strong driving force on the proton motion in the region from Glu278 to its final destination, which has no correspondence in the situation on the left. The reason immediate reprotonation is unlikely to occur in the TS on the right is that the proton which is at the pump-site at this stage has a repulsive effect toward the proton moving in the D-channel toward Glu278. This repulsion does not exist in the first case since there is no proton at the pump-site at that stage; see further discussion on this point below.

In the following, the two types of TSs shown in Figure 5, will be investigated for the pumping mechanism. In particular, proton motion from the N-side to the pump-site will be compared to the one from the N-side to the BNC. As in the previous study,[5] a process is concluded to be allowed at the timescale of milliseconds for the pumping process if the barrier is $\leq$14 kcal/mol, while it is not allowed if the barrier is $\geq$16 kcal/mol. At certain points, also a barrier below 16 kcal/mol can be accepted for a nonpumping step, if it competes with a pumping step with a sufficiently lower barrier. In order to make a quantitative analysis, the distances shown in Figure 6 will here be used together with a dielectric constant of 3.3. The Coulombic interaction energies given in parenthesis in the figure are then obtained. The effects on the barrier of the second type of TS, the one on the right in Figure 5, are also needed. For this reason, the position of the proton in the TS is chosen as about half the distance between Glu278 and BNC. An electron on heme a will then have a small stabilizing effect on the barrier of about 2 kcal/mol, and a proton on Prop-A will instead have a destabilizing effect of about the same size. In contrast to these rather small effects, an electron on the BNC has a large stabilizing effect of about 8 kcal/mol on the TS. A few comments should be made already at this stage. The positions of the charges involved in the electrostatic evaluations are put at the points indicated in the figure. These exact positions can obviously be questioned, especially for the electrons where the charge in reality is somewhat spread out. This fact, together with possibilities to use a somewhat different ϵ value, means that there are certain flexibilities in the exact interpretations of the processes. Still, the accuracy of the present procedure is believed to be at least as high as is presently obtainable using a more detailed electrostatic picture or using a quantum model of the electronic structure (see further discussion on this point in the Conclusions).

Before the presently suggested mechanism is discussed in detail, the above interaction energies will be used to show that, for proton motion to the pump-site, a neutral TS such as the one to the right in Figure 5 is not possible if proton leakage back to the N-side should be avoided. The experimental barrier for proton transfer to the pump-site (**3** in Figure 3) would be 12.2 kcal/mol using transition state theory for a charge-neutral TS which is not affected by pH, in a reaction that is exergonic by -5.0 kcal/mol (derived in the previous study from experiments). This leads to a barrier in the backward direction of 17.2 kcal/mol. At this stage, there is an uncompensated negative charge on heme a. Later on in the cycle, the negative charge is compensated (**6** in Figure 3). When the negative charge is removed there will be a destabilization of the energy for the proton on the pump-site by $+7.1$ kcal/mol, but essentially no effect on the neutral TS. The barrier for the backward reaction will therefore be lowered to $(17.2 - 7.1) = 10.1$ kcal/mol. This barrier is too low to prevent back-leakage, since the rate-limiting barrier in the forward direction is 13.9 kcal/mol, and there would be no pumping. In contrast, with a positively charged TS, the proton at the pump-site and the TS will be destabilized by about the same amount when the effect of the electron is removed. As discussed in the Introduction, the experimental value for a positively charged TS is 10.8 kcal/mol, yielding a barrier in the backward direction of $(10.8 + 5.0) = 15.8$ kcal/mol. Thus, the back-leakage barrier in this case will be 15.8 kcal/mol, which is enough for forcing the proton to be pumped. A more detailed estimate of this barrier is given below.

It should also be added that a positively charged TS for both proton transfers, to the pump-site and to the BNC, is not possible either, as mentioned above. This follows directly from the

interaction energy between the pump-site and Glu278 and the fact that there is already a proton at the pump-site when the proton is going to the BNC. If the barrier is 10.8 kcal/mol, as measured for the transfer to the pump-site when there is no initial proton at this site, it would be raised by 6.1 kcal/mol to (10.8 + 6.1) = 16.9 kcal/mol with a proton at the pump-site. Such a barrier would make the chemistry too slow, and therefore, there would be no proton pumping.

The conclusion reached from the above simple considerations is thus that the transition state has to change character between the two different proton transfers, the one to the pump-site and the one to the BNC. There are two major reasons for having such a change. The first one has already been discussed in detail and concerns the presence or absence of a proton at the pump-site. Even more important is the position of the electron. Although the energy for taking a proton from the N-side to Glu278 is strongly affected by the presence of an electron on heme a (see above), proton transfer from Glu278 to the pump-site is essentially independent of the presence of this electron, since the distance from heme a to Glu278 and the pump-site is about the same; see Figure 6. The effect of the electron in the BNC on the motion between Glu278 and the BNC is completely different. In this case, the proton is moving directly toward the electron, which therefore contributes a large driving force to the charge separation process. This is the key difference exploited in the discussion below.

In Figure 7, the barrier heights for the two types of transition states discussed above are shown for different stages of the pumping sequence. The energies in the diagrams are obtained in the following way. Case **A** represents the situation when the first proton from the N-side should go to the pump-site with an electron on heme a. According to the previous study, a TS of the type to the left in the figure should be passed and the barrier is obtained from the kinetic experiments[4] and transition state theory as 10.8 kcal/mol at pH = 7. The reaction was in the previous study chosen to be exergonic by −5.0 kcal/mol to match experimental observations. Case **B** describes the situation when the second proton is taken up from the N-side and goes to the BNC with the electron at BNC. At this stage, a proton is at the pump-site, and its repulsion toward the proton coming up through the D-channel leads to the choice of the second type of TS, to the right in the figure. The barrier from experiments is 13.2 kcal/mol, and the exergonicity −3.9 kcal/mol (from the previous study and experiments). With these choices, the barrier in case **A** using the TS structure to the right becomes 17.2 kcal/mol. This is obtained by taking 13.2 kcal/mol from case **B** for this TS, first adding 8.0 kcal/mol since the electron is removed from the BNC, then subtracting 2.0 kcal/mol since the destabilization from the proton on Prop-A is removed from **B**, and subtracting another 2.0 kcal/mol since the stabilizing effect of an electron on heme a is added. The final result for the barrier to the right in case **A** is then (13.2 + 8.0 − 2.0 − 2.0) = 17.2 kcal/mol. The reaction energy for this diagram is not needed. Similarly, the barrier for the TS to the left in case **B** is obtained as (10.8 + 6.1 + 7.4 − 8.2) = 16.1 kcal/mol from the interaction energies given in Figure 6. The conclusions from cases **A** and **B** is that it is a consistent assumption that the proton transfer will use a charged TS with barrier 10.8 kcal/mol for the first proton moving to the pump-site in case **A**, and that a neutral TS with barrier 13.2 kcal/mol will be chosen for the second proton moving to the BNC in case **B**.

The rest of the energies in the diagrams will be a check that the above two TS structures are consistent with experimental observations. Situation **C** in Figure 7 represents an important

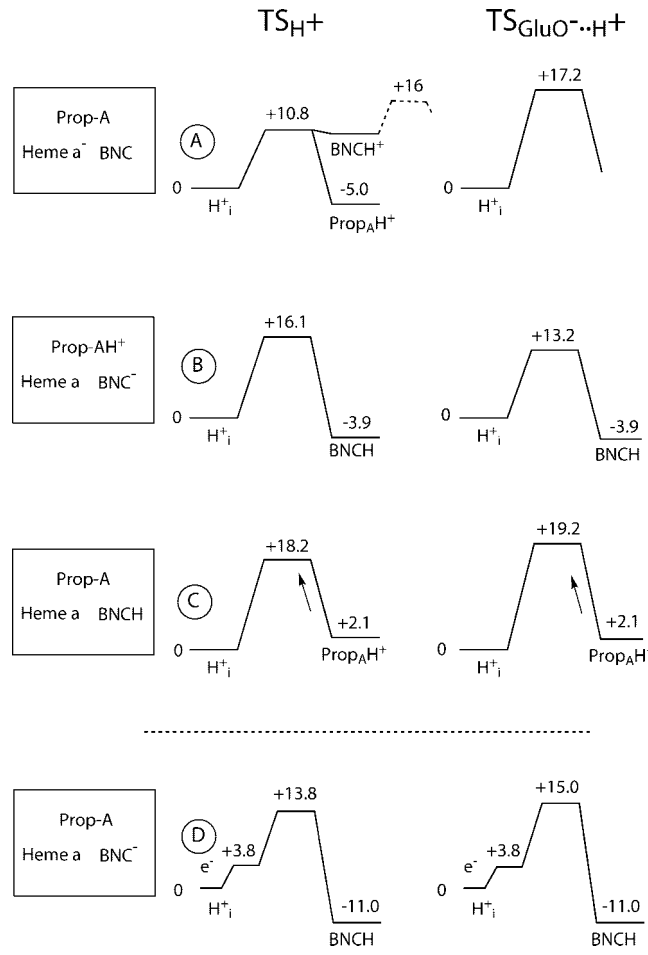

Figure 7. Presently suggested model for pumping. Each diagram shows the reactant and the product and the character of the transition state. The diagrams on the left have a charged TS with GluOH···H_3O^+, while those on the right are neutral with a charge separation of GluOH into $GluO^-$ and H_3O^+. Compare with Figure 5.

stage of proton pumping where a proton is at the pump-site, and both a proton and an electron has reached the BNC. The diagrams in **C** should therefore be read backward. The critical question here is if both types of TS will have large enough backward barriers to prevent back-leakage. In other words, if any one of the TS structures would have a too low barrier, it would be used for back-leakage. The forward barrier for the positively charged TS, to the left in the figure, is obtained from the one in **A** of 10.8 kcal/mol (experimentally determined), by adding +7.4 kcal/mol which corresponds to the lowering effect of the electron on heme a on the TS at Glu278. In the same way, the reaction energy is obtained starting from −5.0 kcal/mol in **A** and adding 7.1 kcal/mol, which is the stabilizing effect of the electron on heme a on the proton on the pump-site. This gives a barrier of (10.8 + 7.4) = +18.2 kcal/mol and a reaction energy of (−5.0 + 7.1) = +2.1 kcal/mol in the forward direction. The important back-leakage barrier is therefore (18.2 − 2.1) = +16.1 kcal/mol, which is ≥16 kcal/mol and therefore fulfills the criterion of being nonallowed. (Note that in the preliminary discussion above a more approximate estimate was made leading to a barrier height of +15.8 kcal/mol.) The reaction energy for the TS to the right in **C** is obtained in the same way as for the one to the left in **A** to be +2.1 kcal/mol. The forward barrier is obtained from the one to the right in **B** of 13.2 kcal/mol by removing the attractive effect of the electron on the BNC in **B** of 8.0 kcal/mol and subtracting the destabilizing effect of 2.0 kcal/mol on the TS by a proton on the pump-

site. Note that the proton on the pump-site is not present for the reactant in this diagram. Therefore, the barrier compared to the reactant is (13.2 + 8.0 − 2.0) = 19.2 kcal/mol and the reaction energy (−5.0 + 7.1) = +2.1 kcal/mol. The back-leakage barrier therefore becomes (19.2 − 2.1) = 17.1 kcal/mol, which is ≥16 kcal/mol as required. It can finally be noted that the forward reaction in **C** also corresponds to the situation before an electron has reached heme a. The diagrams then show that in this situation there will be no proton transfers, since the forward barriers are ≥16 kcal/mol.

The appearance of a back-leakage barrier which is ≥16 kcal/mol for the TS to the right in **C** may appear confusing in light of the initial discussion above where this type of TS was shown to be inadequate for preventing backflow. There is in fact no conflict here, and the difference in the conclusions is only due to different assumptions of starting points. On the right in **C**, the barrier was derived on the assumption that the neutral TS is used only for the protons going to the BNC. For protons going to the pump-site, a charged TS, such as on the left in **A**, was assumed. If it had instead been assumed that the TS used for proton motion to the pump-site in **A** was neutral as to the right, the barrier to the right in **C** would be 12.2 kcal/mol (experimentally measured for **A** and pH independent), since the effect of the electron on heme a would be minor. The leakage barrier would then be (12.2 − 2.1) = 10.1 kcal/mol which is far too small to prevent leakage. In other words, pumping would not work if the two TS, the one for motion to the pump-site and the one to the BNC, were both neutral. This is why two different characters of the transition states were assumed here. It is, of course, also necessary that the different characters of the TS make chemical sense and that each TS is optimal for that particular situation. As discussed above, the different types of TS follow naturally from the different conditions in **A** and **B**.

The situation appearing in **D** is also of high importance for pumping. In this case, an electron has reached the BNC before the proton has reached the pump-site. This situation must be avoided since a proton from the N-side would then prefer to go directly to the BNC, and there would be no pumping. From the previous study, an electron transfer from heme a to the BNC was set to +3.8 kcal/mol. The barrier for the positively charged TS to the left for a proton going to the BNC would then be (3.8 + 10.8 + 7.4 − 8.2) = 13.8 kcal/mol, taking into account that the electron has left heme a (see **A**) and moved to the BNC. This pathway, which would not lead to pumping is thus 3 kcal/mol higher than the competing step to the left in **A** which is the desired step, leading to pumping. This energy difference corresponds to a leakage of 1%, which should be acceptable. For the pathway using a neutral TS, as to the right, the barrier from the intermediate at +3.8 kcal/mol is obtained by taking the barrier from the right in **B** and subtract the repulsive effect of the (absent) proton on the pump-site. The barrier becomes (3.8 + 13.2 − 2.0) = 15.0 kcal/mol. Thus, this pathway, with a barrier 4.2 kcal/mol higher than the pumping pathway, should also be sufficiently prevented.

The final situation discussed here is the one to the left in **A** where a proton has passed the positively charged TS but goes to the BNC rather than to the desired pump-site. At this stage, there is no electron at the BNC and the transfer is therefore substantially endergonic as indicated in the diagram. Furthermore, there is a barrier for the following electron transfer from heme a to the BNC. The solution suggested here for preventing this pathway, which would not lead to pumping, is therefore that the sum of the endergonicity of the proton transfer to the BNC and the following barrier for the electron transfer is ≥16 kcal/mol. Precisely how this energy should be divided into its two components requires more detailed calculations. A large endergonicity for the proton transfer is supported by previous quantum mechanical calculations.[17]

A final minor comment should be made about the character of the neutral TS. In Figure 5, this TS is shown with a proton being on the way from the N-side to Glu278. It is quite possible that this proton has reached all the way to Glu278 in the actual TS. It is important to emphasize that this could only happen if the distance between $GluO^-$ and the proton being on the way to the BNC is quite large. With only a small charge separation, the TS will behave essentially as positively charged and the barrier will be too large due to the presence of the proton on the pump-site.

IV. Proton Motion in the Binuclear Center

The reduction of molecular oxygen in cytochrome c oxidase occurs in four steps, each involving the uptake of one electron and one proton for the chemistry, together with the translocation of one proton across the membrane. The chemistry occurs at the binuclear center. Two proton channels connecting the binuclear center with the inside of the membrane have been identified in the crystal structure of the protein, the D- and the K-channels. The D-channel is used for all protons pumped, and also for at least the first two chemical protons taken up after O_2 is bound to the BNC, i.e., during the oxidative part of the catalytic cycle. There is experimental evidence that during the second part of the cycle, the reductive part, one or maybe both chemical protons are taken up via the K-channel,[36,37] which ends in the vicinity of the tyrosine residue in the binuclear center (see Figure 4). One important question that has to be answered to fully understand the mechanism of proton pumping is why there are two proton channels, i.e. what is the function of the K-channel and what forces this channel to be used instead of the D-channel at certain points of the catalytic cycle? Another interesting experimental observation is that the oxidized intermediate **O**, formed after the oxidative part of the cycle, can be found in two different forms.[38] The oxidized intermediate formed in the previous step pumps protons in the reductive part of the catalytic cycle if it is immediately reduced, while a relaxed form of the oxidized state, referred to as the resting form, does not pump protons upon reduction.[38] It is therefore interesting to investigate possible variations in the structure of the oxidized intermediate that could correspond to the active and the resting form. For proton motion to occur in the binuclear center, water molecules will play an important role, and therefore, the binding energies of water molecules in the BNC need to be examined. The catalytic effect of a water molecule in a similar heme containing active site has previously been described for P450.[39]

One possible form of the **O** intermediate is shown in Figure 4 with $Fe(III)-OH_2$, Cu(II)−OH, and tyrosinate. The tyrosine residue, cross-linked to one of the histidine ligands of copper, is believed to be involved in the O−O bond cleavage step, donating a proton and an electron to molecular oxygen, resulting in a neutral tyrosyl radical. The electron is immediately replaced in the next step, eliminating the radical, while it is not clear when the proton is replaced. Therefore, most of the intermediates of the catalytic cycle can have either a neutral tyrosine or a negative tyrosinate, and consequently, there are two possibilities for the number of protons on the two metal-bound oxygens. Thus, an alternative form of the **O** intermediate would be Fe(III)−OH, Cu(II)−OH, and tyrosine. These two forms of compound **O**, the one with a tyrosinate and the one with a tyrosine, could correspond to the active and the resting form

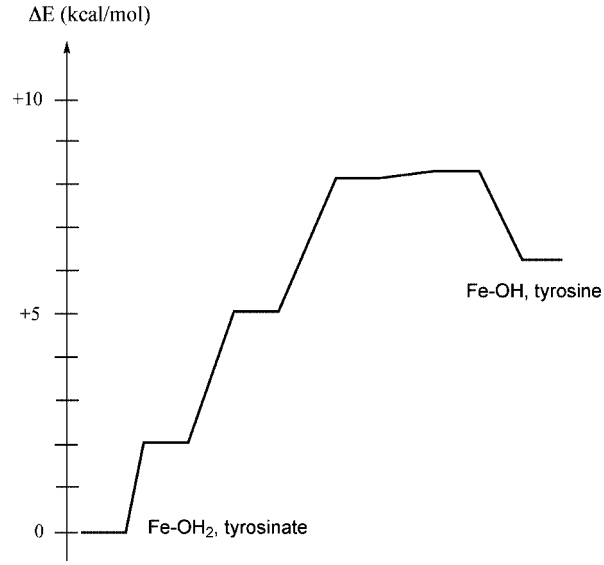

Figure 8. Calculated potential energy surface for proton motion from the W_2 water molecule to the tyrosinate in the **O** state. See Figure 4.

observed experimentally.[38,40] However, to explain the experimental observations there must be a high barrier to go from the resting to the active form, i.e. for proton motion within the binuclear center, preventing the reformation of the active form. Furthermore, a high barrier for proton transfer within the binuclear center at certain points of the catalytic cycle could explain the role of the K-channel, since such a barrier might inhibit the reprotonation of the tyrosinate via the D-channel.

To shed some light on the questions discussed above, calculations were performed using the model in Figure 4 to investigate the energetics of proton motion between the iron bound oxygen (W_2) and the tyrosinate. In this model, which was used before to study the O−O bond cleavage step,[27] an extra water molecule has been inserted, W_3, between the tyrosinate and the iron-bound water. This extra water molecule is a prerequisite for making it possible for a proton to alternate between the two sites. A second extra water molecule was also included in the model, but it was found to be unbound relative to bulk water at this stage of the catalytic cycle, and it was therefore omitted in the investigations reported here. In the calculations of the binding energy relative to bulk water, a standard value of 14 kcal/mol is used for the binding energy of one water molecule in bulk water. The calculated energy profile for proton motion within the binuclear center in the intermediate state **O** is shown in Figure 8. From the figure, it can be seen that the tyrosinate structure is about 6 kcal/mol lower in energy than the tyrosine structure. This is essentially an effect of a change in binding energy of the inserted water molecule (W_3), since without this water molecule, the two structures differ by less than 1 kcal/mol. However, as can be seen from Table 1, where the computed binding energies of different water molecules in different intermediates of the reductive part of the catalytic cycle relative to bulk water are collected, the extra water molecule (W_3) is still bound by a few kilocalories per mole (11.5−6) in the tyrosine structure. The proton motion described in Figure 8 is not a concerted reaction moving the two protons involved at the same time, but rather a stepwise process, where the relative energies have been calculated for different frozen O−H distances. The highest point on the potential energy surface is about 8 kcal/mol above the reactant, indicating that the barrier for proton motion is not prohibitively high. The structure of the highest point corresponds to having moved a W_2 proton all the way to W_3 and with a W_3 proton approaching the tyrosinate. The relative energies along the proton motion path at the B3LYP and the B3LYP* levels are almost identical, within a couple of tenths of a kilocalorie per mole.

TABLE 1: Calculated Binding Energies for Water Molecules in the Binuclear Center, Relative to Bulk Water (in kilocalories per mole) for Different Intermediate States[a]

state of BNC	no. of water molecules	W_1	W_2	W_3
O: Cu(II)OH,	2		20.8 (23.2)	11.5 (11.0)
Fe(III)OH_2	1	11.3 (13.0)	9.9 (13.5)	
E: Cu(I)OH_2,	3	0.6 (1.4)	11.4 (12.5)	10.0 (10.9)
Fe(III)OH_2	2		13.0 (15.3)	13.2 (14.4)
	1		−1.0 (0.2)	−0.9 (−0.8)
$\mathbf{E}_R$: Cu(I)OH_2,	3	2.8 (3.8)	3.1 (6.6)	8.8 (10.2)
Fe(II)OH_2	2	3.1 (4.8)	3.4 (7.1)	5.4 (6.6)
	1	−4.1 (−5.6)	−1.7 (1.9)	0.7 (1.0)

[a] All states are in the tyrosinate form. B3LYP* values are given in parenthesis. The numbering of the water molecules is given in Figure 4. The binding energy of one water molecule to bulk water is assumed to be 14 kcal/mol.

As mentioned above, for proton transfer to occur between different parts of the binuclear center, it is necessary to have some bound water molecules. An alternative explanation for the need of the K-channel could be that the water molecules, the extra one or the newly formed ones, are not bound at later stages of the reductive part of the catalytic cycle, thus inhibiting proton transfer from the D-channel to the tyrosinate. Therefore, the binding energy of all water molecules present in the binuclear center were computed for the intermediates labeled **O**, **E**, and $\mathbf{E}_R$, and the results are collected in Table 1. The **E** state is formed from the **O** state by adding one electron and one proton, and the $\mathbf{E}_R$ state is formed from the **E** state by adding one electron only. The results presented in the table are obtained with the tyrosinate form for all states. In the **O** state, with Cu(II) and Fe(III) and one hydroxyl group, the extra water W_3 is bound by 11.5 kcal/mol relative to bulk water, and the water molecule on iron W_2 is bound by as much as 20.8 kcal/mol. However, if the W_3 molecule is removed, the binding energy of W_2 decreases to 9.9 kcal/mol, showing that there is a strong cooperative effect in the binding of the water molecules. If the hydroxyl group instead is moved to iron, the binding energy of the water molecule on copper in the single water case is quite similar, 11.3 kcal/mol. In the **E** state, with Cu(I), Fe(III), and three water molecules, the W_1 molecule is just barely bound relative to bulk, and it has actually left its coordination to copper. Water W_2 and W_3 are about equally strongly bound, by 10−11 kcal/mol. The same is true if W_1 is removed leaving only two water molecules in the BNC, increasing the binding energy slightly to 13 kcal/mol per water. Again, the cooperative effect of the two water molecules is very strong, such that if any of the two water molecules are removed, the remaining single water molecule is actually unbound by about 1 kcal/mol relative to bulk water. Finally, when also iron is reduced (to Fe(II)), giving rise to the $\mathbf{E}_R$ state, the binding energies of the water molecules are generally decreased, in particular that of W_2. There is still a cooperative effect, such that with two or three water molecules in the BNC they are all bound with a few kcal/mol relative to bulk water, while a single water molecule is slightly unbound

whatever its position. The values of the binding energies mentioned in the text are the B3LYP values, while in Table 1 also the B3LYP* values are given. As can be seen in the table, the B3LYP* values are rather similar to the B3LYP values and give the same qualitative picture. For the W_1 and W_2 molecules, the B3LYP and B3LYP* binding energies differ by less than 2 kcal/mol, while for the W_3 molecule the difference is somewhat larger, typically between 2 and 4 kcal/mol. A larger difference between the B3LYP and B3LYP* values is expected for the W_3 water because when this molecule is removed the spin state on the iron atom changes from low spin to high spin.

In conclusion, no obstacle was found for proton transfer within the binuclear center, neither in terms of high barriers nor in terms of lack of bound water molecules. However, it should be noted that these results could depend on the choice of model. At least two missing factors in the model might affect the barrier height for the proton transfer. One factor is that there is one amino acid not included in the model but which is close enough to the BNC to have an effect on the possibility for the water molecules to bind in the way they are doing in the present model. This amino acid is a valine which is peptide linked directly to the tyrosine included in the model and which has the side chain pointing toward Cu_B. It does not collide with the positions of the water molecules in the present model, but it is close enough to enforce changes in the structure. Calculations have been started with a larger model including this valine. Another aspect of the present model is the fact that the tyrosine residue might be too free to move since it is only restricted by the covalent bonding to the histidine. In the new model also, the peptide link between tyrosine and the valine is included, which will reduce the mobility of the tyrosine side chain and which might prevent the strong bonding of the water molecules in the binuclear center.

V. Conclusions

Two different problems in the proton pumping mechanism of cytochrome c oxidase have been addressed in the present study. The first problem concerns the direct mechanism for proton pumping. A solution was presented in an earlier paper[5] for why protons are forced to the P-side against the membrane gradient. An electrostatic gating involving a positively charged TS as shown in Figure 3 was shown to give the desired result. However, a problem was noted to match the experimental rate for proton transfer to the BNC. A solution to this problem has been suggested here by using a more flexible type of TS as shown in Figure 5, leading to potential curves schematically shown in Figure 7. It was demonstrated that agreement with the kinetic experiments[4] was obtained and that pumping is achieved in the desired way. Future modeling work is required for obtaining more atomistic details about the proton transfer pathways, and the presently suggested TS should be very useful in this context.

In the quantum chemical modeling part of the present study, proton transfer through the BNC was investigated with three water molecules present. It was shown that proton transfer is relatively easy and that the required water molecules are bound with respect to the bulk. Therefore, the calculations did not give any additional clues as to why the K-channel appears to be necessary in the reductive part of the cycle. Calculations are in progress using a larger model of the active site with more constraints from the X-ray structure to see if these modifications will change the conclusions.

The present paper is an illustration of the fact that different problems require different methods. Even though the conclusions and argumentations for the pumping mechanism are based on a very simple electrostatic picture, the investigation still requires that the experimental results are strictly followed. One might ask if it would not be desirable to study this problem with a more sophisticated method than has been done here. The simple answer advocated here is that a straightforward application of a quantum mechanical/molecular mechanical (QM/MM) approach would not be possible in a meaningful way since the error bars would be too large. The extremely important advantage with the present approach is that accurate experimental barriers can be built directly into the analysis. On the other hand, the present approach could be improved if the experimental data were used as a calibration of a QM/MM study, and this is therefore one obvious continuation of the present study.

References and Notes

(1) Wikström, M. K. F. *Nature* **1977**, *266*, 271–273.
(2) Yoshikawa, S.; Shinzawa-Itoh, K.; Nakashima, R.; Yaono, R.; Yamashita, E.; Inoue, N.; Yao, M.; Fei, M. J.; Libeu, C. P.; Mizushima, T.; Yamaguchi, H.; Tomizaki, T.; Tsukihara, T. *Science* **1998**, *280*, 1723–1729.
(3) Ostermeier, C.; Harrenga, A.; Ermler, U.; Michel, H. *Proc. Natl. Acad. Sci., USA* **1997**, *94*, 10547–10553.
(4) Belevich, I.; Bloch, D. A.; Belevich, N.; Wikström, M.; Verkhovsky, M. I. *Proc. Natl. Acad. Sci. USA* **2007**, *104*, 2685–2690.
(5) Siegbahn, P. E. M.; Blomberg, M. R. A. *Biochim. Biophys. Acta* **2007**, *1767*, 1143–1156.
(6) Verkhovsky, M. I.; Wikström, M. *Biochim. Biophys. Acta* **2007**, *1767*, 1200–1214.
(7) (a) Morgan, J. E.; Verkhovsky, M. I.; Wikström, M. *J. Bioenerg. Biomembr.* **1994**, *26*, 599–608. (b) Wikström, M.; Morgan, J. E.; Verkhovsky, M. I. *J. Bioenerg. Biomembr.* **1998**, *30*, 139–145. (c) Wikström, M. *Biochim. Biophys. Acta* **2000**, *44827*, 1–11.
(8) (a) Michel, H. *Proc. Natl. Acad. Sci. USA* **1998**, *95*, 12819–12824. (b) Michel, H. *Biochemistry* **1999**, *38*, 15129–15140. (c) Ruitenberg, M.; Kannt, A.; Bamberg, E.; Fendler, K.; Michel, H. *Nature* **2002**, *417*, 99–102.
(9) Gennis, R. B. *Proc. Natl. Acad. Sci. USA* **1998**, *95*, 12747–12749.
(10) Mitchell, R.; Rich, P. R. *Biochim. Biophys. Acta* **1994**, *1186*, 19–26.
(11) Capitanio, N.; Vygodina, T. V.; Capitanio, G.; Konstantinov, A. A.; Nicholls, P.; Papa, S. *Biochim. Biophys. Acta* **1997**, *1318*, 255–265.
(12) Blair, D. F.; Ellis, J.; Walther, R.; Wang, H.; Gray, H. B.; Chan, S. I. *J. Biol. Chem.* **1986**, *261*, 1524–1537.
(13) Carithers, R. P.; Palmer, G. *J. Biol. Chem.* **1981**, *256*, 7967–7976.
(14) Artzatbanov, V. Y.; Konstantinov, A. A.; Skulachev, V. P. *FEBS Lett.* **1978**, *87*, 180–185.
(15) Brzezinski, P.; Larsson, G. *Biochim. Biophys. Acta* **2003**, *1605*, 1–13.
(16) Faxen, K.; Gilderson, G.; Ädelroth, P.; Brzezinski, P. *Nature* **2005**, *437*, 286–289.
(17) Siegbahn, P. E. M.; Blomberg, M. R. A.; Blomberg, M. L. *J. Phys. Chem. B* **2003**, *107*, 10946–10955.
(18) Siegbahn, P. E. M.; Blomberg, M. R. A. In *Biophysical and Structural Aspects of Bioenergetics*; Wikström, M., Ed.; Royal Society of Chemistry: Cambridge, UK, 2005; 99−122.
(19) Blomberg, M. R. A.; Siegbahn, P. E. M. *J. Comp. Chem.* **2006**, *27*, 1373–1384.
(20) Popovic, D. M.; Stuchebrukhov, A. A. *FEBS Lett.* **2004**, *566*, 126–130.
(21) Medvevev, D. M.; Medvevev, E. S.; Kotelnikov, A. I.; Stuchebrukhov, A. A. *Biochim. Biophys. Acta* **2005**, *1710*, 47–56.
(22) Popovic, D. M.; Stuchebrukhov, A. A. *J. Phys. Chem. B* **2005**, *109*, 1999–2006.
(23) Olsson, M. H.; Sharma, P. K.; Warshel, A. *FEBS Lett.* **2005**, *579*, 2026–2034.
(24) Olsson, M. H.; Warshel, *Proc. Natl. Acad. Sci. USA* **2006**, *103*, 6500–6505.
(25) Olsson, M. H.; Siegbahn, P. E. M.; Blomberg, M. R. A.; Warshel, A. *Biochim. Biophys. Acta* **2007**, *1767*, 244–260.
(26) Song, Y.; Michonova-Alexova, E.; Gunner, M. R. *Biochemistry* **2006**, *45*, 7959–7975.
(27) Blomberg, M. R. A.; Siegbahn, P. E. M.; Wikström, M. *Inorg. Chem.* **2003**, *42*, 5231–43.
(28) Blomberg, M. R. A.; Siegbahn, P. E. M. *Biochim. Biophys. Acta* **2006**, *1757*, 969–980.
(29) *Jaguar 5.5*; Schrödinger, L. L. C., Portland, OR, 1991−2003.

(30) Tannor, D. J.; Marten, B.; Murphy, R.; Friesner, R. A.; Sitkoff, D.; Nicholls, A.; Ringnalda, M.; Goddard, W. A., III.; Honig, B. *J. Am. Chem. Soc.* **1994**, *116*, 11875–11882.

(31) Marten, B.; Kim, K.; Cortis, C.; Friesner, R. A.; Murphy, R. B.; Ringnalda, M.; Sitkoff, D.; Honig, B. *J. Biol. Chem.* **1996**, *100*, 11775–11788.

(32) Curtiss, L. A.; Raghavachari, K.; Redfern, R. C.; Pople, J. A. *J. Chem. Phys.* **2000**, *112*, 7374–83.

(33) Siegbahn, P. E. M.; Blomberg, M. R. A. *Annu. Rev. Phys. Chem.* **1999**, *50*, 221–249.

(34) Reiher, M.; Salomon, O.; Hess, B. A. *Theor. Chem. Acc.* **2001**, *107*, 48–55.

(35) Salomon, O.; Reiher, M.; Hess, B. A. *J. Chem. Phys.* **2002**, *117*, 4729–4737.

(36) Wikström, M.; Jasaitis, A.; Backgren, C.; Puustinen, A.; Verkhovsky, M. I. *Biochim. Biophys. Acta* **2000**, *1459*, 514–520.

(37) Ruitenberg, M.; Kannt, A.; Bamberg, E.; Ludwig, B.; Michel, H.; Fendler, K. *Proc. Natl. Acad. Sci. USA* **2000**, *97*, 4632–4636.

(38) Bloch, D. A.; Belevich, N.; Jasaitis, A.; Ribacka, C.; Puustinen, A.; Verkhovsky, M. I.; Wikström, M. *Proc. Natl. Acad. Sci. USA* **2004**, *101*, 529–533.

(39) Altun, A.; Shaik, S.; Thiel, W. *J. Comp. Chem.* **2006**, *27*, 1324–1337.

(40) Kaukonen, M. *J. Phys. Chem. B* **2007**, *111*, 12543–12550.

JP801635C